Heliyon 11 (2025) e41226

Contents lists available at ScienceDirect

Heliyon

journal homepage: www.cell.com/heliyon

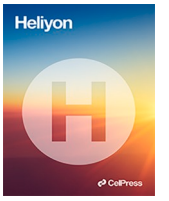

Research article

A potential eco-friendly degradation of methyl orange by water-ball (sodium polyacrylate) stabilized zero valent iron nanoparticles

Saud Bawazeer

Department of Pharmaceutical Science, Faculty of Pharmacy, Umm Al-Qura University, Makkah, P.O. Box 751, Saudi Arabia

ARTICLE INFO

Keywords:
Water balls
Fe NPs
MO degradation
Statistical analysis
Kinetic study

ABSTRACT

This study presents the synthesis and application of water-ball (sodium polyacrylate) stabilized zero-valent iron nanoparticles (wb@Fe^0) for the eco-friendly degradation of Methyl Orange (MO). The nanoparticles were prepared using a chemical reduction method using $NaBH_4$. Characterization techniques including Field Emission Scanning Electron Microscopy (FESEM), Energy Dispersive X-ray Spectroscopy (EDS), Fourier Transform Infrared Spectroscopy (FTIR), X-ray Photoelectron Spectroscopy (XPS), and X-ray Diffraction (XRD) were employed to analyze the morphology, elemental composition, valent state and crystallinity of the nanoparticles. The catalytic performance was evaluated under standard conditions, with a maximum degradation efficiency of 94 % achieved for a 0.05 mM MO solution using 10 mg of the catalyst, 0.1 mM $NaBH_4$, at neutral pH and room temperature within 10 min. Optimal degradation occurred at 40 °C and pH 6. The catalyst demonstrated excellent recyclability, maintaining activity over ten reuse cycles. Kinetic studies revealed that the degradation followed first-order kinetics with an R^2 value of 0.8907 and a rate constant of 0.3708. Though with a lower R^2 value (0.6884), the second-order kinetics model indicated the highest rate constant of 2.6522. Regression and ANOVA analysis confirmed the accuracy of the reaction protocol. This study highlights the potential of water-ball stabilized zero-valent iron nanoparticles for effective dye pollutant removal and degradation, offering a promising approach for environmental remediation.

1. Introduction

In the present era, environmental pollution has emerged as a significant challenge, and its remediation has become a top priority for modern science [1]. One of the basic fundamental rights of every individual is access to safe water; however, unhygienic water causes around 80 % of health problems [2]. Industries contribute significantly to water pollution by discharging a large number of organic and inorganic materials into the surrounding water, with organic materials primarily consisting of phenolic compounds and dyes. These pollutants pose a significant threat to the health of human beings and other living organisms [3–5].

Several approaches have been developed for wastewater treatment, including adsorption, filtration, membrane technology, and advanced oxidation methods such as photocatalysis [6,7]. However, these techniques face several challenges, including high cost, low efficacy, by-product formation, and their tedious nature. Despite these challenges, research continues to find effective and efficient ways to treat wastewater and remediate environmental pollution caused by organic pollutants [8–10]. The development of new

E-mail address: ssbawazeer@uqu.edu.sa.

https://doi.org/10.1016/j.heliyon.2024.e41226
Received 28 June 2024; Received in revised form 12 November 2024; Accepted 12 December 2024
Available online 15 December 2024

materials and technologies that are cost-effective, efficient, and environmentally friendly is a critical area of focus in this field [11–14].

Iron nanoparticles (NPs) have attracted considerable attention in recent years because of their significant applications in varieties of fields, such as water treatment, environmental remediation, and medical sciences [15–17]. Iron NPs have been extensively studied for their catalytic performance in the detoxification of different organic pollutants [18,19]. The zero-valent iron (ZVI) nanoparticles have shown outstanding catalytic activity in the degradation of different organic pollutants, including dyes [20]. However, their practical application is limited due to the aggregation and agglomeration of NPs in aqueous media. To overcome this issue, various stabilizing agents have been used, such as surfactants, polymers, and natural materials [20,21]. Recently, super absorbent polymers (SAPs) have been used as stabilizing agents for iron NPs due to their ability to absorb and retain large amounts of water. Waterballs, a type of SAP, have been used as stabilizing agents for metal NPs [22]. Waterballs are highly hydrophilic and can absorb up to 300 times their weight in water. They have been used in various fields, like drug delivery, tissue engineering, and the removal of environmental remediation. Water balls are effective and easily available materials, reflecting its significance as a readily available stabilizing agent for metallic NPs. This leads to improved catalytic performance and reusability of the nanoparticles [22,23].

Dye pollutants are a major source of environmental contamination, particularly in developing countries where textile industries are growing rapidly [24–26]. Methyl orange is a common dye pollutant that is difficult to degrade due to its complex chemical structure [27]. It is known to be toxic to aquatic organisms such as fish, algae, and invertebrates. Exposure to even low concentrations of methyl orange can disrupt aquatic ecosystems, leading to reduced biodiversity and ecological imbalances. Furthermore, methyl orange has been identified as a potential carcinogen and mutagen, posing risks to human health through exposure via contaminated water sources or food chains. Prolonged exposure to methyl orange may cause adverse health effects such as skin irritation, respiratory issues, and organ damage [28].

Therefore, the removal of methyl orange from contaminated water sources is necessary to mitigate its harmful effects on both the environment and human health. Effective removal methods must be employed to treat wastewater and prevent the discharge of methyl orange into natural water bodies. Various methods have been used for the degradation of methyl orange, including biological, chemical, and physical methods [29–31]. Among these, the use of iron nanoparticles (NPs) has shown promising results due to their high surface area, reactivity, and low cost [32]. The use of iron NPs for the degradation of methyl orange has shown promising results. Iron NPs can catalyze the degradation of methyl orange by reducing it to simpler and less toxic compounds.

The focus of our research is on using water-ball (sodium polyacrylate) as a stabilizing agent for zero-valent iron nanoparticles (ZVI-NPs). While various stabilizers have been used previously, the application of water balls represent a novel approach that offers significant improvements in nanoparticle stability and dispersion in aqueous solutions. This approach mitigates common issues related to NP aggregation, enhancing the efficiency and practicality of the catalyst. Our study demonstrates that the water-ball stabilized ZVI-NPs exhibit superior performance in the degradation of Methyl Orange compared to previously reported methods. This includes a rapid degradation rate and high efficiency, which are critical for effective wastewater treatment. The use of water-balls not only provides a cost-effective stabilizing solution but also aligns with eco-friendly practices. The material is biodegradable and readily available, making it a sustainable choice for large-scale applications. These contributions represent meaningful advancements in the field of environmental remediation and highlight the practical benefits of our approach.

The main objective of this study is to stabilize iron NPs using water balls and test their efficiency for the degradation of methyl orange. The study will include synthesizing and characterizing iron NPs stabilized with water balls. The results of this study will provide insight into the potential application of water balls as stabilizing agents for iron NPs in environmental remediation.

2. Experimental

2.1. Materials and methods

2.1.1. Chemicals and reagents

Methyl orange (MO) was obtained from BDH, while iron (III) chloride hexahydrate ($FeCl_3{\cdot}6H2O$) was obtained from Sigma Aldrich. Deionized water was used in all the experiments. The iron nanoparticles (NPs) were prepared by the reduction of $FeCl_3$ using sodium borohydride ($NaBH_4$) as a reducing agent. The waterballs (sodium polyacrylate) used as stabilizing agents for the iron NPs were obtained from a commercial source. The analytical-grade chemicals and reagents utilized in the investigation were employed without additional purification.

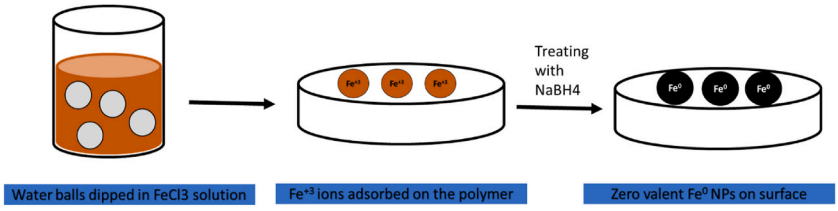

Scheme-1. Schematic representation of the formation of supported zero-valent Fe NPs.

2.1.2. Water balls supported zero-valent Fe NPs

To prepare the water balls-supported zero-valent iron (ZVI) NPs, 1 g of water balls were washed thoroughly with distilled water to remove any suspended dust and impurities. The cleaned water balls (2 g) were then immersed in 200 mL of 0.1 M concentrated solution of iron (III) chloride ($FeCl_3$) for 24 h at room temperature to allow the uptake of metal ions onto their surfaces. Afterward, the water balls were taken out from the salt solution and washed with deionized water to remove any excess salt. Next, the water balls were treated with freshly prepared 1 mM sodium borohydride ($NaBH_4$) solution to reduce the iron ions to the zero-valent state [20]. The reduction to the zero-valent state of iron ions was confirmed by a change in the color of the water balls to black as shown in the inset of **Scheme-1**.

2.1.3. Catalytic performance

The catalytic performance of wb@Fe^0 was investigated for the degradation of MO dye. The initial concentration and volume of MO dye were 0.05 mM and 2.5 mL respectively. The reduction reaction was observed using UV–Vis spectroscopy. 2.5 mL from the MO solution and 0.5 mL with a concentration of 0.1 mM $NaBH_4$ solution were combined with 10 mg of the appropriate catalyst for the time-dependent absorbance spectrum tests. A UV–Vis spectrophotometer was then used to analyze the reaction mixture. The reaction was carried out at room temperature and neutral pH.

2.1.4. Instrumentation

The morphological characteristics of the prepared catalysts were examined with a field emission-scanning electron microscope (JEOL JSM-7600F, Japan), and their elemental makeup was validated using energy dispersive X-ray spectrometry (EDS). Fourier-transformed infrared spectroscopy (Thermo Scientific FT-IR spectrometer) was used to explore the functional groups responsible for stabilizing zero-valent Fe NPs in the water balls. The X-ray Photoelectron Spectroscopy (XPS) analysis of the polymer-stabilized zerovalent iron nanoparticles reveals key insights into the surface chemistry and composition of the material While XRD was used to confirm the crystallinity. The time-dependent double-beam UV–visible spectrophotometer (Model UV-2601) was used to analyze the degradation process.

3. Results and discussion

3.1. FTIR

The FTIR spectra of both the beard water balls and loaded Fe NPs were recorded to investigate the functional groups involved in stabilizing the NPs. A clear peak was observed at 3350 cm^{-1}, corresponding to the -OH group [33]. However, peak broadening was observed in the Wb@Fe sample, which may be due to the development of hydrogen bonding. Another peek at 1640 cm-1 was observed in both samples, representing the presence of carboxylic functional groups [22]. These functional groups interact with the NPs and immobilize them to increase stability. The FTIR spectra of the beard water balls and Wb@Fe NPs are shown in Fig. 1.

3.2. FESEM

The field emission scanning electron micrograph is a powerful tool for investigating the surface morphology of the NPs. We take FESEM images of the wb@Fe^0 NPs at high and low resolution. The FESEM image shows the porous structure which responsible for the stabilization of metallic NPs. The water balls surface morphology feature makes it suitable for the adsorption of metal ions and ultimately stabilized it by the implication of $NaBH_4$. The FESEM images are provided in the inset of Fig. 2.

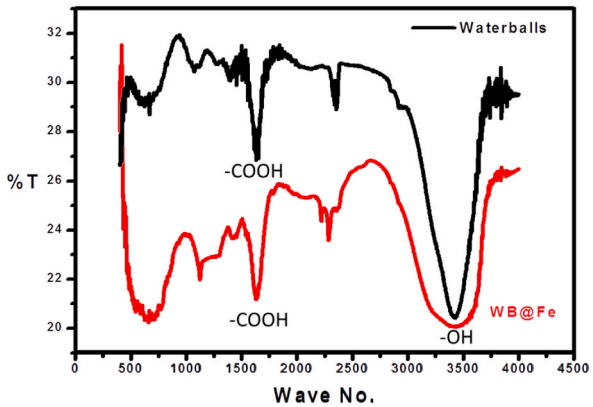

Fig. 1. FTIR spectrum of beard water balls and wb@Fe^0.

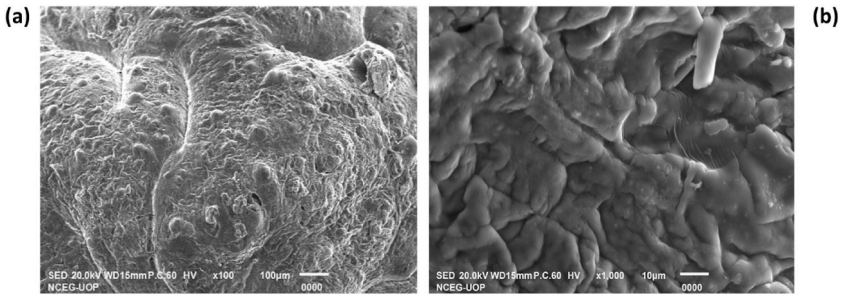

Fig. 2. FESEM images of wb@Fe0 NPs (a) Low resolution (b) High Resolution.

3.3. EDS

The elemental analysis of the prepared catalysts was carried out via electron dispersive spectroscopy (EDS). EDS is a powerful tool for investigating the elemental composition. The EDS spectrum of the synthesized catalyst shows that the catalyst has Carbon at up to 12.06 %, Oxygen at 57.13 % and Fe was 15.89 %. This indicates its purity. The EDS spectrum is shown in Fig. 3.

3.4. XPS analysis

The X-ray Photoelectron Spectroscopy (XPS) analysis of the polymer-stabilized zerovalent iron nanoparticles reveals key insights into the surface chemistry and composition of the material. The binding energies recorded in the C 1s, O 1s, and Fe 2p regions provide evidence for the presence of carbon, oxygen, and iron, respectively. The C 1s peaks at 284.8 eV and 286.5 eV correspond to the carbon atoms within the polymer matrix. The intensity values suggest a significant carbon presence, which is expected given the polymer's organic nature. The O 1s peaks at 530.2 eV and 532.0 eV are indicative of oxygen species associated with the polymer, likely from carbonyl or hydroxyl groups, further confirming the presence of oxygen-containing functional groups in the stabilizing polymer. The Fe 2p region, showing distinct peaks at 707.0 eV confirms the presence of zerovalent iron in the nanoparticles. The binding energies observed for these peaks are consistent with those typically attributed to Fe^0, indicating that the iron within the nanoparticles is predominantly in its zerovalent state. The intensity of these peaks suggests that iron is well-dispersed and abundant within the sample, further supporting the successful synthesis and stabilization of zerovalent iron nanoparticles by the polymer as shown in the inset of Fig. 4a.

3.5. XRD

The XRD pattern of the freshly synthesized wb@Fe^0 is presented in Fig. 4b. The results reveal that iron predominantly exists in its zero-valent state (Fe^o), as indicated by the primary diffraction peak at a 2θ value of 44.9°. Additional peaks were observed at 65.22° and 82.50°, corresponding to the body-centered cubic (bcc) crystal structure of Fe^o, specifically the (110), (200), and (211) lattice planes, respectively [34].

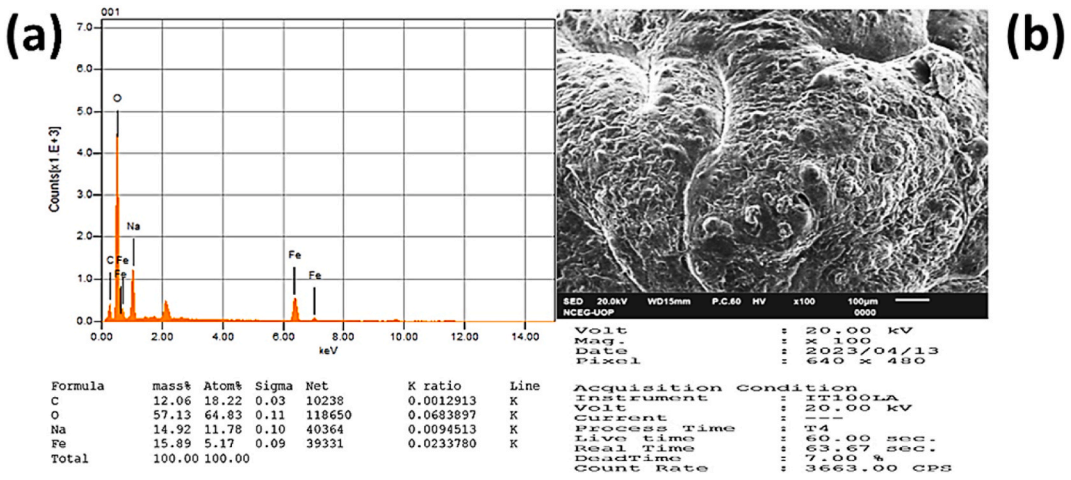

Fig. 3. EDS spectrum of wb@Fe^0 NPs.

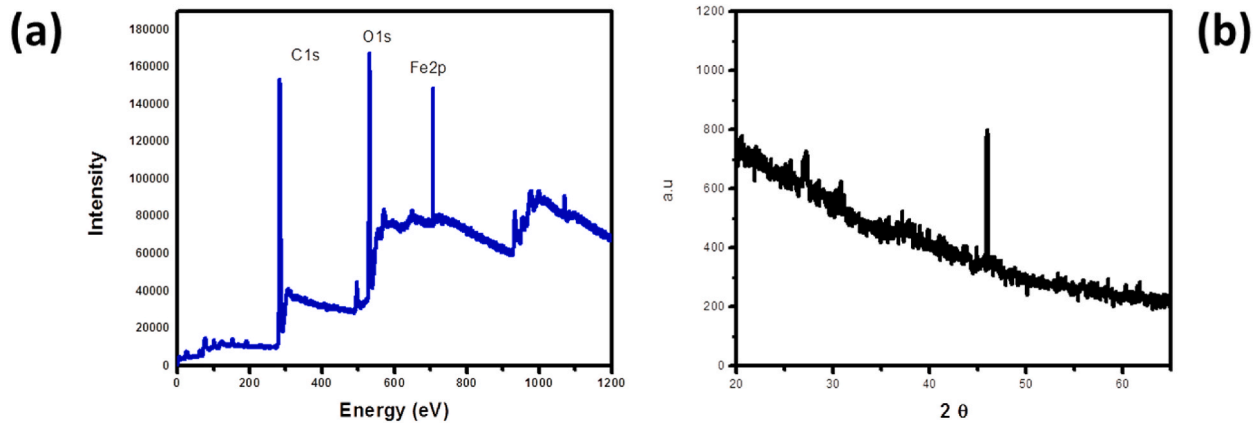

Fig. 4. The XPS and XRD spectra of wb@Fe^0

3.6. *Catalytic evaluation against the degradation of MO*

For the catalytic evaluation of the prepared catalysts, we subjected the wb@Fe^0 catalyst to the degradation of MO. Firstly, 2.5 mL of 0.05 mM of MO was taken in a cuvette and its parent spectra were recorded using a UV–visible spectrophotometer. Next, 0.5 mL of 0.1 mM NaBH4 was freshly prepared and added to the mixture. The spectra were recorded again to establish a baseline. Subsequently, 10 mg of the stated catalyst was subjected to the reaction mixture, and spectra were recorded in a UV–visible spectrophotometer. We

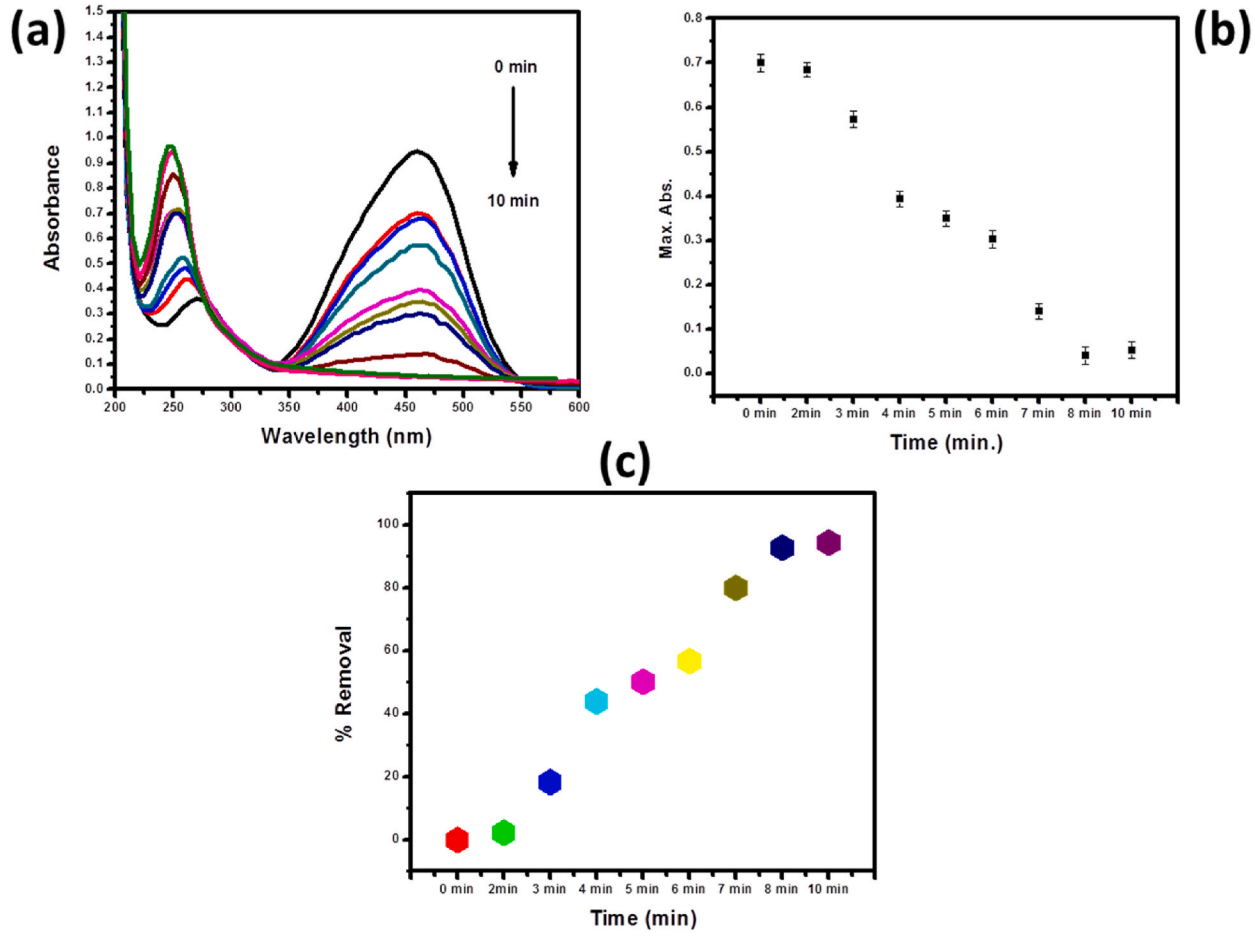

Fig. 5. Degradation of MO Via wb@Fe^0 (a), with standard error (b) and percent removal (c).

observed a change in color and a decrease in lambda max, which confirmed the degradation of MO.

After removing the catalyst from the reaction mixture, we used the following formula to determine the percentage of dye removal:

$$\text{Removal efficiency} = \frac{C_o - Ct}{C_o} \times 100 \quad (1)$$

Where C_o is the initial concentration of MO, and Ct is the concentration of MO after the reaction.

Our results indicate that the wb@Fe^0 catalyst showed excellent catalytic activity towards the degradation of MO. The catalyst was able to achieve a high percent removal efficiency, demonstrating its potential as a promising candidate for wastewater treatment applications.

3.6.1. Degradation of MO

In aqueous media, Methyl orange (MO) showed two different absorption bands. The first band was observed at 260 nm due to the presence of the pi to pi* transition in the aromatic ring, while the existence of a nitrogen-based chromophore caused the n to pi* transition, which caused the second band to form at 464 nm. The catalytic potential of the synthesized catalyst was assessed using the absorbance maxima corresponding to the azo group at 464 nm [35].

For this purpose, the wb@Fe^0 catalyst was evaluated by testing its catalytic activity against the degradation of MO. In the reaction, 2.5 mL of 0.05 mM MO was taken in a UV cuvette with a maximum wavelength at 460 nm, and then 0.5 mL of 0.1 mM freshly prepared NaBH4 was added to it. After that, 10 mg of the wb@Fe^0 catalyst was added, and the UV–visible spectral data for the entire reaction was recorded until the peak disappeared. The absorption peak at 464 nm progressively vanished with time. Due to the breakdown of the azo functional group of MO and the production of the amino (-NH_2) group, there was a noticeable blue shift at 250 nm and the orange color disappeared. The possible mechanism for the sequestration and reduction process involves the adsorption of the reducing agent ($NaBH_4$) onto the surface of the nanocatalyst. As a result, the electrons and hydrogen atoms that have been adsorbed on the surface of Fe^0 nanoparticles are moved to the pollutant that is being reduced or degraded. The final degraded product of MO is N,N-dimethyl-p-phenylenediamine, which is a colorless compound [20,21,32,35,36].

The overall degradation reaction can be represented as follows:

$$MO + NaBH_4 + 2H_2O + \text{wb@Fe0 catalyst} \rightarrow N,N-\text{dimethyl}-p-\text{phenylenediamine} + NaBO_2 + 4H_2 \quad (2)$$

Our results showed that the wb@Fe^0 catalyst was highly effective in degrading MO, achieving a degradation efficiency of 94 % in just 10 min (Fig. 5). This indicates that the wb@Fe^0 catalyst is a promising candidate for the treatment of wastewater contaminated with MO.

Moreover, the high degradation efficiency achieved by the wb@Fe^0 catalyst can be attributed to the unique structure of the catalyst. The catalyst consists of Fe^0 nanoparticles supported on polymer, which provide a porous and stable matrix for the nanoparticles. The porous structure allows for a high degree of accessibility to the active sites on the Fe^0 nanoparticles, enabling efficient contact between the catalyst and the dye molecules [22,23].

The comparison of our results with existing literature, as outlined in **Table -1**, provides valuable insights into the performance of different catalysts for the removal of targeted pollutants. The table includes data on various catalysts and their effectiveness in degrading MO and other pollutants, highlighting both removal times and references to relevant studies. Our work, which utilizes the wb@Fe^0 catalyst, demonstrates a removal time of 10 min for MO. This result is notable when compared to other catalysts listed in the table. For instance, the ZV-Fe NPs catalyst achieved a removal time of 100 min indicating that wb@Fe0_00 significantly outperforms this catalyst in terms of reaction speed. On the other hand, catalysts such as Co/MA and Ni/MA showed much shorter removal times of 4.5 min and 8 min, respectively. These catalysts, though effective, often involve more complex or costly synthesis methods compared to wb@Fe^0 (see Table 2).

3.6.2. Degradation mechanism

According to the literature, the degradation of azo dyes like MO using metallic nanoparticles such as zero-valent iron nanoparticles (ZVI-NPs) in the presence of a reducing agent like sodium borohydride is a multi-step process that involves surface adsorption, electron transfer, and subsequent reduction reactions. The process begins with the adsorption of both the dye molecules and the reducing agent onto the surface of the ZVI-NPs. The catalyst surface plays a crucial role by providing active sites that facilitate the adsorption of the reactants, allowing them to interact more effectively [38–40]. In terms of mechanism, the dye and $NaBH_4$ are absorbed on the catalyst's surface, which causes the atoms on the surface of the MNPs to rearrange themselves. To ensure the reduction process, it's also

Table-1
Comparison of the present work with the literature.

S.NO	Catalyst	Targeted Pollutants	Removal time (min.)	Reference
1	ZV-Fe NPs	MO	100	[37]
	Co/MA		4.5	[21]
	Ni/MA		8	
	MA@Ag		10	[36]
	ACA@Fe^0		8	[20]
	wb@Fe^0		10	This work

Table-2
Different kinetics models for the degradation of MO.

Kinetics Model	Rate Constant (k)	Correlation coefficient (R^2)
1st Order	0.3708	0.8907
Pseudo 1st order	0.3708	0.8907
2nd Order	2.6522	0.6884

feasible that hydrogen atoms adsorb on catalyst surfaces. The dyes were transformed into their derivatives with the addition of $NaBH_4$, however, the discoloration was caused by the use of catalysts [21]. During the reaction, the reducing agent $NaBH_4$ is first adsorbed onto the surface of the zerovalent iron nanoparticles, where it generates hydrogen gas and hydride ions (BH_4^-). The hydride ions then react with the surface of the MNP's to transfer electrons to the targeted contaminant, which in this case is Methyl orange. The electrons are used to reduce the azo group (-N=N-) of Methyl orange. The reduction of the azo group leads to the formation of amino ($–NH_2$) groups, which are colorless [35,41–43].

Furthermore, these degraded MO derivatives, primarily aniline, and N, N-dimethylaniline, may undergo secondary degradation processes. Depending on the reaction conditions, these products can be further transformed through hydrolysis, oxidation, or photodegradation, potentially leading to the formation of completely harmless end products like carbon dioxide, water, and other simple organic molecules [35,44]. Moreover, the efficiency of this degradation process can be influenced by several factors. The pH of the solution, the temperature, and the concentration of both the catalyst and the dye play significant roles in determining the rate and extent of degradation. For example, at a lower pH, the concentration of hydride ions is higher, which can enhance the reduction process, leading to faster decolorization. Similarly, increasing the temperature can accelerate the reaction by providing the necessary activation energy, while an optimal catalyst dose ensures maximum surface area for adsorption and electron transfer. The generalized schematic representation of the MO degradation has been provided in the inset of Scheme 2.

3.6.3. Kinetic study

Kinetics studies are an essential aspect of chemical reactions as they help to determine the rate and mechanistic pathway of chemical reactions. In this particular study, different kinetic models were used to study the degradation of MO. The first-order kinetic model, which assumes that the rate of the reaction is proportional to the reactant concentration, gave a high correlation coefficient (R^2) of 0.8907 and a rate constant of 0.3708 (Fig. 6 a). The pseudo-first order kinetics model, which is used when the reaction involves multiple reactants, also gave a similar correlation coefficient and rate constant (Fig. 6 b). However, the second-order kinetic model, which assumes that the rate of the reaction is proportional to the square of the concentration of the reactant, gave a lower correlation coefficient (R^2) of 0.6884 and a higher rate constant of 2.6522 as shown in Fig. 6c.

The obtained results suggest that the degradation of MO follows a 1st-order kinetics model as the rate constant obtained from the 1st-order and pseudo-first-order kinetics models is the same, while the rate constant obtained from the 2nd-order kinetics model is much higher. The high correlation coefficient obtained from the 1st-order and pseudo-first-order kinetics models indicates that the second-order kinetics model is not as well-fitting to the experimental data as these models are.

Therefore, the first-order kinetics model can be used to accurately predict the rate of degradation of MO under similar reaction conditions. The data regarding kinetic studies is tabulated in the inset of **Tabl-2.**

3.7. Effect of catalyst dose, temperature, pH and dye concentration

To optimize the degradation process, we investigated the effects of catalyst dose, temperature, pH, and dye concentration.

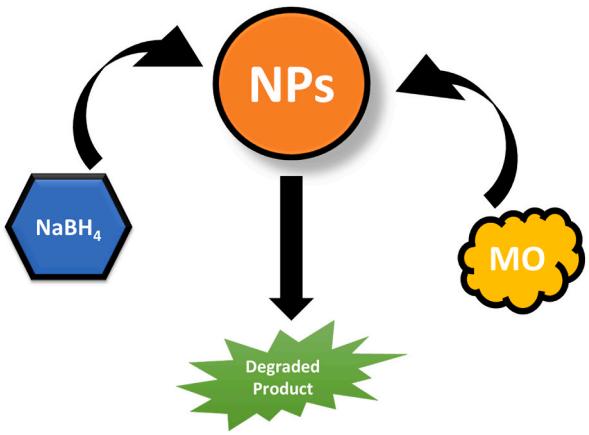

Scheme 2. Generalized representation of MO degradation.

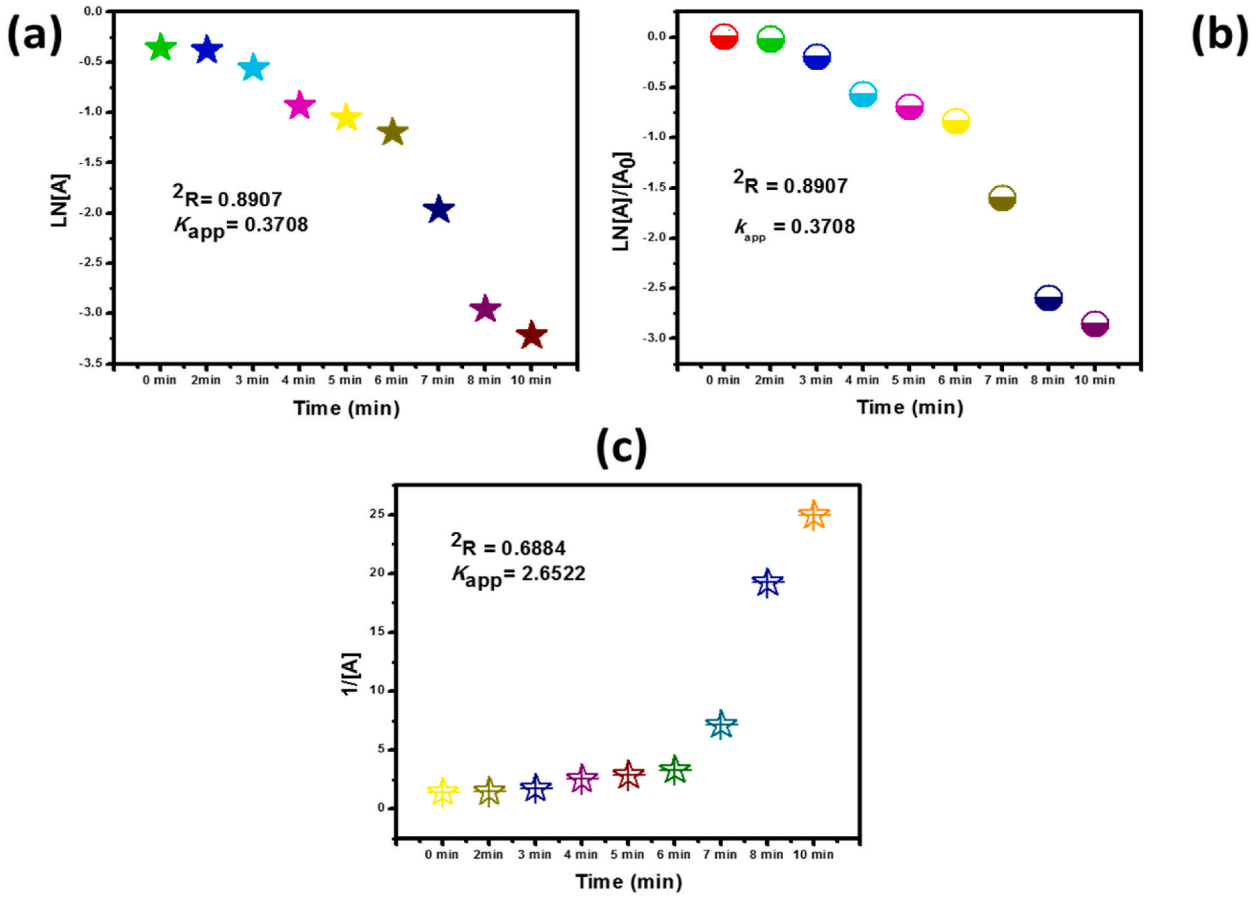

Fig. 6. 1st order (a), Pseudo-1st order (b) and 2nd order kinetics (c) of MO degradation using wb@Fe^0

Increasing the catalyst dose to 15 mg, while keeping the dye concentration and other conditions constant, resulted in a 96 % degradation of MO in 10 min (Fig. 7a). This enhancement is consistent with previous studies, which suggest that a higher catalyst dose provides more active sites for the degradation process, thus increasing the reaction rate [45]. Raising the temperature to 40 °C further improved the degradation efficiency, achieving 96.6 % degradation of MO in just 8 min (Fig. 7b). This effect aligns with reports indicating that higher temperatures accelerate the reaction rate by enhancing the kinetic energy of the reacting molecules. Similarly, lowering the pH to 6 resulted in the highest degradation of MO, up to 96.92 % in 7 min (Fig. 7c). This finding is supported by previous research, which indicates that pH affects the charge and solubility of both the catalyst and dye, optimizing the reaction conditions [46]. The effect of dye concentration was also notable. Doubling the dye concentration led to a slight decrease in degradation efficiency, with 94.6 % degradation observed in 12 min (Fig. 7d). This result is in line with studies showing that higher dye concentrations can result in competition for active sites on the catalyst, reducing overall efficiency. Overall, our investigation demonstrates that maximum degradation of MO is achieved at pH 6, corroborating the findings of previous studies and providing a comprehensive understanding of the impact of each parameter.

3.8. Recyclability

Recyclability is one of the main issues in the catalytic degradation of organic pollutants. Usually, the catalyst becomes inactive after the first or second use due to fouling, poisoning, or structural changes. However, in this work, the catalyst demonstrated remarkable reusability, maintaining activity over ten cycles. Fig. 8 illustrates the performance of the catalyst across ten cycles of reuse. Initially, during the first cycle, the catalyst achieved an impressive 96 % degradation of Methyl Orange (MO) within just 10 min, highlighting its high efficiency and rapid catalytic activity. This substantial initial performance underscores the catalyst's effectiveness in breaking down MO. As shown in Fig. 7, a gradual decline in catalytic activity is evident as the number of cycles increases. By the 6th cycle, the catalyst's degradation efficiency decreased to 80 %, indicating a noticeable reduction in activity. By the 10th cycle, the degradation efficiency further declined to 60.51 %, and the time required for complete degradation extended to 1 h. This trend of decreasing efficiency over successive cycles suggests that while the catalyst retains its functionality, its performance diminishes with repeated use. This investigation highlights the potential of the catalyst for repeated use in practical applications, Factors contributing to the decrease in activity could include catalyst surface fouling, loss of active sites, or structural changes, which should be addressed to enhance long-

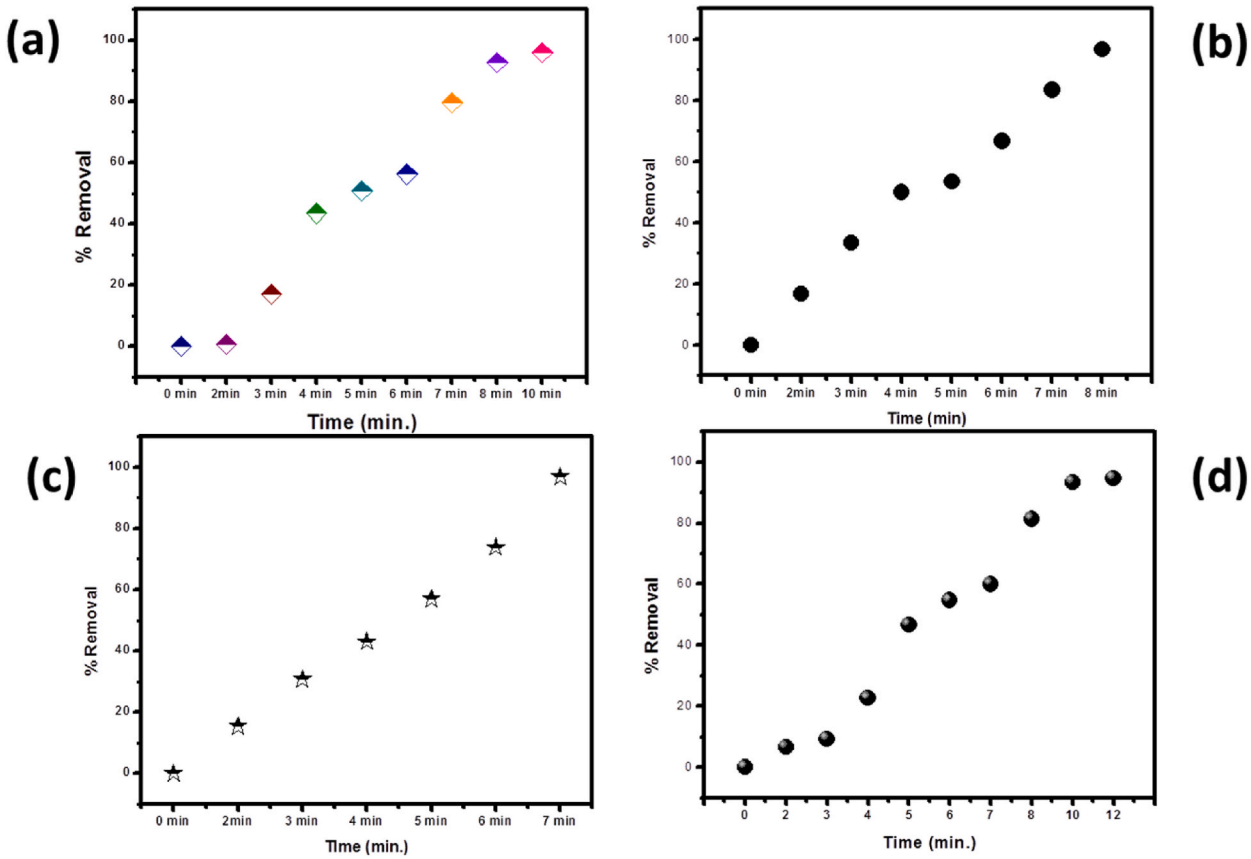

Fig. 7. Effect of catalyst dose (a), Temperature (b) pH (c) and dye concentration (d) of MO degradation using wb@Fe^0

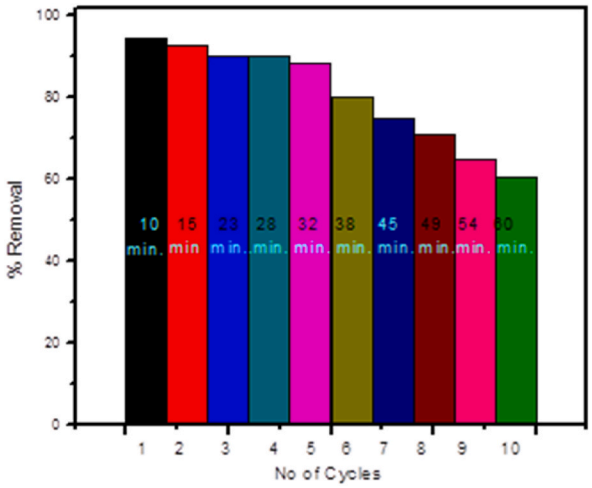

Fig. 8. Recyclability of synthesized catalyst.

term performance.

3.9. Regression and ANOVA analysis

The regression analysis demonstrates a significant negative linear relationship between time and absorbance values, with an R^2 value of 0.956. This high R^2 value indicates that the linear regression model explains 95.6 % of the variance in the absorbance data,

suggesting that time is a critical factor influencing the degradation of MO. The steep decline in absorbance over time corresponds to the ongoing breakdown of MO, facilitated by the catalytic activity of the metallic nanoparticles (NPs) in the presence of $NaBH_4$.

The ANOVA results show a statistically significant difference in the mean absorbance values at different time points ($F = 28.259$, $p < 0.05$). The significant F-statistic, coupled with a p-value less than 0.05, confirms that the degradation process is not random but strongly time-dependent. This suggests that the reaction progresses effectively over time, supporting the hypothesis that the metallic NPs are highly effective in catalyzing the degradation of MO when combined with $NaBH_4$.

The regression analysis and ANOVA both validate the data and reaction protocol for the degradation of MO using metallic NPs in the presence of $NaBH_4$. The significant negative linear relationship between time and absorbance values, as shown by the high R^2 value, indicates that time has a strong effect on the degradation of MO. The significant difference between the means of the absorbance values at different time points, as shown by the low p-value, indicates that the reaction protocol is effective in degrading MO. Therefore, both the regression analysis and ANOVA represent the validation and significance of the data and reaction protocol.

4. Conclusion

The study demonstrates the synthesis and characterization of water-ball stabilized zero valent iron NPs and their efficacy in the degradation of Methyl Orange as a model dye pollutant. The results indicate a 94 % degradation efficiency with the addition of 10 mg of the catalyst and NaBH4 as a reducing agent. Various kinetics models were employed, and the first-order kinetics model was found to be the best fitting model with a rate constant of 0.3708. The regression and analysis of variance (ANOVA) validated the reaction protocol, indicating high accuracy. Overall, the synthesized water-ball stabilized zero valent iron nanoparticles show potential for efficient removal and degradation of methyl orange, making them a promising eco-friendly solution.

Data availability statement

Data included in article/supp. material is referenced in the article.

Additional information

No additional information available in this paper.

Funding

None.

Declaration of competing interest

The authors declare that they have no known competing financial interests or personal relationships that could have appeared to influence the work reported in this paper.

Acknowledgment

The author is greatly acknowledging the Department of Pharmaceutical Science, Faculty of Pharmacy, Umm Al-Qura University, Makkah for providing experimental facilities.

References

[1] M. Bilal, T. Rasheed, H.M. Iqbal, Y. Yan, Peroxidases-assisted removal of environmentally-related hazardous pollutants with reference to the reaction mechanisms of industrial dyes, Sci. Total Environ. 644 (2018) 1–13.
[2] R. Qadri, M.A. Faiq, Freshwater pollution: effects on aquatic life and human health, Fresh Water Pollution Dynamics and Remediation (2020) 15–26.
[3] S. Jodeh, O. Hamed, A. Melhem, R. Salghi, D. Jodeh, K. Azzaoui, Y. Benmassaoud, K. Murtada, Magnetic nanocellulose from olive industry solid waste for the effective removal of methylene blue from wastewater, Environ. Sci. Pollut. Control Ser. 25 (2018) 22060–22074.
[4] A.K. Mishra, Application of Nanotechnology in Water Research, John Wiley & Sons, 2014.
[5] A. Muhammad, A. Shafeeq, M. Butt, Z. Rizvi, M. Chughtai, S. Rehman, Decolorization and removal of cod and bodfrom raw and biotreated textile dye bath effluent through advanced oxidation processes (AOPS), Braz. J. Chem. Eng. 25 (2008) 453–459.
[6] S. Kalidhasan, H.-Y. Lee, Preparation of floating PDMS sponge catalysts embedded with copper oxide (s): a prelude to the study of its application toward the effective rhodamine B degradation by sonochemical method, J. Environ. Chem. Eng. 10 (2022) 107254.
[7] S. Kalidhasan, H.-Y. Lee, Preparation of TiO2-deposited silica-based catalysts for photocatalytic decomposition of chloro-pesticide to environmentally less toxic species, Chemosphere 290 (2022) 133300.
[8] S. Kalidhasan, D.-G. Park, K.S. Jin, H.-Y. Lee, Engineered polymer–clay–copper oxides catalyst for the oxidation and reduction of organic molecules: synergy of degradation and instinctive interface stability by polymer self-healing function, Surface. Interfac. 39 (2023) 102934.
[9] S. Kalidhasan, Y.-S. Lim, E.-A. Chu, J. Choi, H.-Y. Lee, Phospholipid-derived Au and Au–Cu suspensions as efficient peroxide and borohydride activators for organic molecules degradation: performance and sustainable catalytic mechanism, Chemosphere 346 (2024) 140567.
[10] D. Vishwakarma, Shikha, Biopolymer-basedmaterials for sustainable water treatment, Journal of Applied Science, Innovation & Technology 1 (2022) 10–14.
[11] S. Guerra-Rodríguez, E. Rodríguez, D.N. Singh, J. Rodríguez-Chueca, Assessment of sulfate radical-based advanced oxidation processes for water and wastewater treatment: a review, Water 10 (2018) 1828.
[12] W. Rudzinski, W. Plazinski, Theoretical description of the kinetics of solute adsorption at heterogeneous solid/solution interfaces: on the possibility of distinguishing between the diffusional and the surface reaction kinetics models, Appl. Surf. Sci. 253 (2007) 5827–5840.

[13] S. Singh, V. Kumar, R. Romero, K. Sharma, J. Singh, Applications of nanoparticles in wastewater treatment, Nanobiotechnology in Bioformulations (2019) 395–418.
[14] J.L. Wang, L.J. Xu, Advanced oxidation processes for wastewater treatment: formation of hydroxyl radical and application, Crit. Rev. Environ. Sci. Technol. 42 (2012) 251–325.
[15] C. Lei, Y. Sun, D.C. Tsang, D. Lin, Environmental transformations and ecological effects of iron-based nanoparticles, Environ. Pollut. 232 (2018) 10–30.
[16] M. Rukhsar, Z. Ahmad, A. Rauf, H. Zeb, M. Ur-Rehman, H.A. Hemeg, An Overview of iron oxide (Fe3O4) nanoparticles: from synthetic strategies, characterization to antibacterial and anticancer applications, Crystals 12 (2022) 1809.
[17] T. Pasinszki, M. Krebsz, Synthesis and application of zero-valent iron nanoparticles in water treatment, environmental remediation, catalysis, and their biological effects, Nanomaterials 10 (2020) 917.
[18] L.-P. Zhang, Z. Liu, Y. Faraj, Y. Zhao, R. Zhuang, R. Xie, X.-J. Ju, W. Wang, L.-Y. Chu, High-flux efficient catalytic membranes incorporated with iron-based Fenton-like catalysts for degradation of organic pollutants, J. Membr. Sci. 573 (2019) 493–503.
[19] H. Gupta, R. Kumar, H.-S. Park, B.-H. Jeon, Photocatalytic efficiency of iron oxide nanoparticles for the degradation of priority pollutant anthracene, Geosystem Engineering 20 (2017) 21–27.
[20] B.O. Aljohny, Z. Ahmad, S.A. Shah, Y. Anwar, S.A. Khan, Cellulose acetate composite films fabricated with zero-valent iron nanoparticles and its use in the degradation of persistent organic pollutants, Appl. Organomet. Chem. 34 (2020) e5892.
[21] Z. Ahmad, S.A. Shah, I. Khattak, H. Ullah, A.A. Khan, R.A. Shah, S.A. Khan, S.B. Khan, Melia Azedarach impregnated Co and Ni zero-valent metal nanoparticles for organic pollutants degradation: validation of experiments through statistical analysis, J. Mater. Sci. Mater. Electron. 31 (2020) 16938–16950.
[22] H.S.M. Ali, S.A. Khan, Stabilization of various zero-valent metal nanoparticles on a superabsorbent polymer for the removal of dyes, nitrophenol, and pathogenic bacteria, ACS Omega 5 (2020) 7379–7391.
[23] Z. Ahmad, S. Salman, S.A. Khan, A. Amin, Z.U. Rahman, Y.O. Al-Ghamdi, K. Akhtar, E.M. Bakhsh, S.B. Khan, Versatility of hydrogels: from synthetic strategies, classification, and properties to biomedical applications, Gels 8 (2022) 167.
[24] Y. Chen, K. Wang, L. Lou, Photodegradation of dye pollutants on silica gel supported TiO2 particles under visible light irradiation, J. Photochem. Photobiol. Chem. 163 (2004) 281–287.
[25] S. Rawat, J. Singh, Degradation of para-nitrophenol by green synthesised iron nanoparticles: optimization of the process parameters and study of degradation kinetics, J. Appl. Sci. Innov. Technol 1 (2022) 21–26.
[26] C. Jin, D. Liu, J. Hu, Y. Wang, Q. Zhang, L. Lv, F. Zhuge, The role of microstructure in piezocatalytic degradation of organic dye pollutants in wastewater, Nano Energy 59 (2019) 372–379.
[27] M.F. Hanafi, N. Sapawe, A review on the water problem associate with organic pollutants derived from phenol, methyl orange, and remazol brilliant blue dyes, Mater. Today: Proc. 31 (2020) A141–A150.
[28] S.K. Dutta, M.K. Amin, J. Ahmed, M. Elias, M. Mahiuddin, Removal of toxic methyl orange by a cost-free and eco-friendly adsorbent: mechanism, phytotoxicity, thermodynamics, and kinetics, South Afr. J. Chem. Eng. 40 (2022) 195–208.
[29] T. Chiong, S.Y. Lau, Z.H. Lek, B.Y. Koh, M.K. Danquah, Enzymatic treatment of methyl orange dye in synthetic wastewater by plant-based peroxidase enzymes, J. Environ. Chem. Eng. 4 (2016) 2500–2509.
[30] Y. Haldorai, J.-J. Shim, An efficient removal of methyl orange dye from aqueous solution by adsorption onto chitosan/MgO composite: a novel reusable adsorbent, Appl. Surf. Sci. 292 (2014) 447–453.
[31] N.A. Youssef, S.A. Shaban, F.A. Ibrahim, A.S. Mahmoud, Degradation of methyl orange using Fenton catalytic reaction, Egyptian Journal of Petroleum 25 (2016) 317–321.
[32] N. Khan, B. Shahida, S.A. Khan, Z. Ahmad, Z. Sheikh, E.M. Bakhsh, H.M. Alraddadi, T.M. Fagieh, S.B. Khan, Anchoring zero-valent Cu and Ni nanoparticles on Carboxymethyl cellulose-polystyrene–block polyisoprene–block polystyrene composite films for nitrophenol reduction and dyes degradation, J. Polym. Environ. 31 (2023) 608–620.
[33] A. Ouass, L. Kadiri, Y. Essaadaoui, R.A. Belakhmima, M. Cherkaoui, A. Lebkiri, R. El Housseine, Removal of trivalent chromium ions from aqueous solutions by Sodium polyacrylate beads, Mediterranean Journal of Chemistry 7 (2018) 125–134.
[34] S. Rk, B. Gangadhar, H. Basu, V. Manisha, N. Grk, Remediation of malathion contaminated soil using zero valent iron nano-particles, Am. J. Anal. Chem. (2012) 2012.
[35] M. Riaz, N. Khan, S.A. Khan, Z. Ahmad, M.A. Khan, M. Iqbal, H.A. Hemeg, E.M. Bakhsh, S.B. Khan, Enhanced catalytic reduction/degradation of organic pollutants and antimicrobial activity with metallic nanoparticles immobilized on copolymer modified with NaY zeolite films, J. Mol. Liq. 359 (2022) 119246.
[36] S.A. Shah, Z. Ahmad, S.A. Khan, Y.O. Al-Ghamdi, E.M. Bakhsh, N. Khan, M. ur Rehman, M. Jabli, S.B. Khan, Biomass impregnated zero-valent Ag and Cu supported-catalyst: evaluation in the reduction of nitrophenol and discoloration of dyes in aqueous medium, J. Organomet. Chem. 938 (2021) 121756.
[37] I.A. Radini, N. Hasan, M.A. Malik, Z. Khan, Biosynthesis of iron nanoparticles using Trigonella foenum-graecum seed extract for photocatalytic methyl orange dye degradation and antibacterial applications, J. Photochem. Photobiol. B Biol. 183 (2018) 154–163.
[38] S.A. Khan, S. Sohni, K. Akhtar, E.M. Bakhsh, T. Nawaz, S.B. Khan, Lignocellulose biomatrix zero-valent cobalt nanoparticles: a dip-catalyst for organic pollutants degradation, Ind. Crop. Prod. 198 (2023) 116694.
[39] H. Sun, S.-Y. Lee, S.-J. Park, Bimetallic CuPd alloy nanoparticles decorated ZnO nanosheets with enhanced photocatalytic degradation of methyl orange dye, J. Colloid Interface Sci. 629 (2023) 87–96.
[40] R.K. Shah, Efficient photocatalytic degradation of methyl orange dye using facilely synthesized α-Fe2O3 nanoparticles, Arab. J. Chem. 16 (2023) 104444.
[41] R. Rajesh, S.S. Kumar, R. Venkatesan, Efficient degradation of azo dyes using Ag and Au nanoparticles stabilized on graphene oxide functionalized with PAMAM dendrimers, New J. Chem. 38 (2014) 1551–1558.
[42] Y.O. Al-Ghamdi, G. Saeed, M. Ali, K. Ali, K. Ullah, N. Khan, M. Iqbal, A.Y. Alzahrani, S.A. Khan, Polymers blended peanuts activated carbon composite hydrogels fabricated Ag NPs as dip-catalyst for industrial dyes discoloration in aqueous medium, Ind. Crop. Prod. 188 (2022) 115588.
[43] R.A. Soomro, A. Nafady, Catalytic reductive degradation of methyl orange using air resilient copper nanostructures, J. Nanomater. 16 (2015), 120-120.
[44] U. Farooq, S. Akter, A. Kaleem Qureshi, H.M. Alhuthali, M. Almehmadi, M. Allahyani, A.A. Alsaiari, A. Aljuaid, M. Farzana, A.Y.M. Alhazmi, Arbutin stabilized silver nanoparticles: synthesis, characterization, and its catalytic activity against different organic dyes, Catalysts 12 (2022) 1602.
[45] P. Bansal, G.R. Chaudhary, S. Mehta, Comparative study of catalytic activity of ZrO2 nanoparticles for sonocatalytic and photocatalytic degradation of cationic and anionic dyes, Chem. Eng. J. 280 (2015) 475–485.
[46] A.N. Chishti, F. Guo, A. Aftab, Z. Ma, Y. Liu, M. Chen, J. Gautam, C. Chen, L. Ni, G. Diao, Synthesis of silver doped Fe3O4/C nanoparticles and its catalytic activities for the degradation and reduction of methylene blue and 4-nitrophenol, Appl. Surf. Sci. 546 (2021) 149070.